Efficient conversion of NO with CeO_2/TiO_2 using non-thermal plasma

Efficient conversion of NO with CeO_2/TiO_2 using non-thermal plasma

George Adwek [1], Boxiong Shen [1,4], Jiancheng Yang [1], Zachary Siagi [2], Jianqiao Wang [1], Kemunto M. Cicilia [1], Moses Arowo [2], Gane Julius [3] and Dongrui Kang [1]

[1] School of Energy and Environmental Engineering, Hebei University of Technology, Tianjin, China;
[2] School of Engineering, Moi University, Eldoret, Kenya;
[3] Energy Research Institute, University of Leeds, LS2 9JT, Leeds, UK.

[4] Email: shenbx@hebut.edu.cn

Abstract. Alternating current (AC) dielectric barrier discharge induced non-thermal plasma (NTP) has been used to experimentally investigate conversion of Nitrogen Oxide (NO) over CeO_2/TiO_2 catalyst. The role of heterogeneous catalyst (TiO_2/CeO_2) has also been investigated, NO conversion has been examined in terms of various operating parameters including temperature, voltage, flue gas flow rate, specific energy density, water vapour content and oxygen content. The conversion mechanism of NO was distinctly discussed. To understand the effects of NTP on CeO_2/TiO_2 catalyst properties and the influence of CeO_2/TiO_2 catalyst on NTP, SEM, BET, XRD, TPR were carried out. SEM reveals that increase in temperature during NTP catalytic reactions affect the morphology of the catalyst hence decreasing NO oxidation efficiency, the results also show that surface area and pore properties of the catalyst plays a significant role in plasma catalytic reaction. The maximum NO oxidation conversion efficiency attained was 93% at SED of $91JL^{-1}$.

1. Introduction

The emissions from combustion flue gas and industrial gases has worsen leading to increase in environmental problems. Coal burning power plants and automobile exhaust result in NOx emissions which are major causes of acidic rainfall. It is unsuitable to apply conventional methods such as lime, gypsum and catalytic reduction methods in treating exhaust gases efficiently and economically, pollution control approach using non- thermal plasmas have been extensively studied since it is part of assured technologies with improved energy efficiencies [1]. In non-thermal plasma the mean energy of electrons is usually higher than that of the ions and the neutrals, providing reasonable benefit by minimizing the energy demand to reduce pollutants [2]. Non thermal plasma generally consists of electrons which are sped up by an electric field, acquiring temperatures in the scope of 10,000-250,000K (1-25ev), and that are not in thermal equilibrium with other particles [3]. Electron molecule collisions with bulk N_2, O_2, H_2O molecules lead to production of excited bulk gas molecules (e.g. N_2^*), followed by excess energy loss and emission of heat or photons. The ions and radicals which are unstable reactive species in oxygen rich surroundings, scavenged and are converted into HO_2^* spontaneously[3]. The most important goal of non- thermal plasma technique is to achieve a discharge in which most of electrical energy is used in energetic electrons production, instead of gas heating, for instance, a common utilization during flue gas cleaning, these electrons produce radicals such as O

and OH, as a result of dissociation and ionization of H_2O or O_2 molecules. Three types of power generators can be used to generate plasma namely; AC, DC and pulse. Pulse and AC energization display a remarkable removal efficiency of nitrogen oxides compared to DC energization. Nonetheless, pulse energization has higher energy efficiency [4-7].

In consideration, to overcome the problems associated with efficiency, cost effectiveness and energy consumption, a combination of non-thermal plasma with suitable catalyst has emerged as a promising mechanism for NO emission control, catalyst selection plays a very important role depending on the nature of the pollutant. The other efficient way to use plasma is possibly by taking advantage of its inherent synergetic potential through combination with heterogeneous catalysts [8-16].

In this work, the plasma-catalytic oxidation of nitrogen oxide (NO) at atmospheric pressure over CeO_2/TiO_2 catalyst from a temperature range of 100^0C ~250^0C flue gas has been investigated using DBD plasma reactor, the effect of CeO_2/TiO_2 catalyst on the plasma-catalytic conversion of NO as a function of specific energy density has been evaluated in terms of NO conversion. Different catalyst characterization techniques, including N_2 adsorption-desorption, temperature programmed reduction by H_2 (H_2-TPR), scanning electronic microscopy (SEM), X-Ray Diffraction (XRD), have been used to demonstrate the links between catalyst properties and NO conversion and for an in-depth understanding of the role of catalyst properties on reaction performance. In order to explain the synergistic effect of NTP- CeO_2/TiO_2 coupling, NO oxidation has been performed using (a) CeO_2/TiO_2 only (b)NTP only (c) NTP-CeO_2/TiO_2 coupling in IPC configuration and results are presented as a function of SED.

2. Experimental section

2.1. Plasma-catalytic system

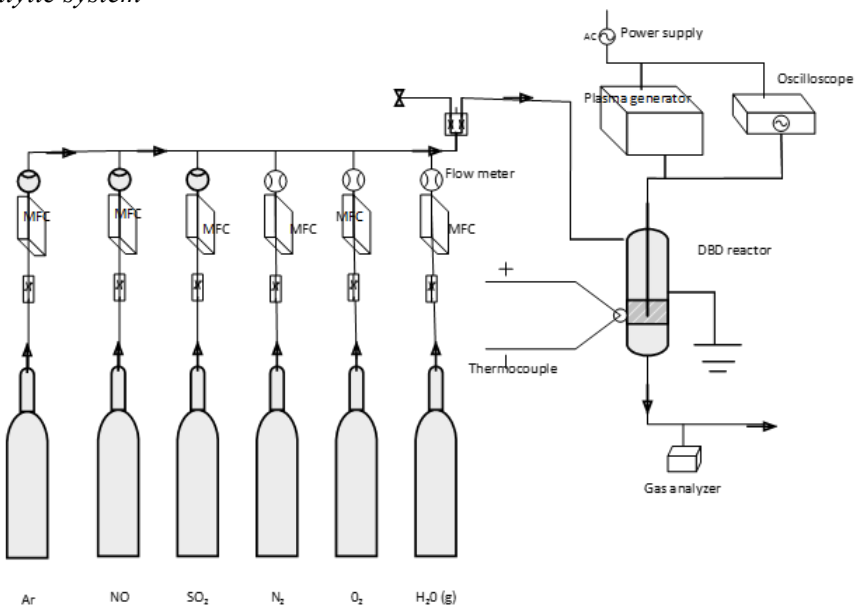

Figure 1. Schematic drawing of the experimental setup.

The experimental setup in Figure. 1 consists of the mass flow controllers, HV power supply, pulse generator, oscilloscope, a plasma catalytic reactor, NO gas analyzer and SO_2 gas analyzer. The gas reactor used was dielectric barrier discharge (DBD) reactor in a cylindrical configuration. It consists of 4mm-diameter tungsten wire as main electrode. The tungsten wire was fixed from the inlet end placed at the centre of 400mm long Pyrex tube using two ceramic rings. The outer surface of the cylinder was wrapped with copper grid and used as a ground electrode. The discharge length was 100mm.

In plasma catalysis (IPC) technique, the catalyst was placed in the discharge zone directly in contact with the discharge and the active species are normally in close proximity with the catalyst surface. The IPC system used modifies the catalyst surface, the catalyst volume of 1ml, 1.5ml, 2ml was placed in the discharge zone using quartz wool. The concentrations of SO_2 and NO were controlled by mass flow controllers (Model MFC-DO71913) while N_2, Ar and O_2 contents of the gas stream were adjusted using flow meters. Keeping the total flow rate constant, H_2O content was controlled by varying the water bath temperature hence changing its vapor pressure.

The plasma-catalyst reactor temperature was increased from 100^0c to 250^0c, with a step size of 50^oC using temperature controller (Model XMTD-7411). The reactor temperature was measured by a K-type thermocouple placed on the reactor surface and the temperature uncertainty was $\pm 2^0$C.The experiment data was recorded at steady state. During the change of temperature from one desired values to the other, the waiting time was at least 25mins for stabilization temperature to be attained. The DBD reactor was driven by CTP-2000K plasma generator (20kV, 200Hz). The output signals were transmitted to Tektronix TDS 2024 oscilloscope having both frequency and voltage display. The concentrations of NO, SO_2, NO_2 and O_2 for all the test runs were continuously monitored by the infrared gas analyzer (KANE-940).

NO and SO_2 conversion was measured in the presence and absence of catalyst, with NTP on/off condition at temperature ranging from 100 ^{o}C to 250^{o}C. In order to get suitable inlet concentration of NO and SO_2, the simulated gases were allowed to flow for 1 hour before the NTP was switched on. The uncertainty was taken into consideration by repeating each experiment three times and the readings were averaged, we concluded that the experimental relative error was less than 0.1, Table 1. Summarizes the detailed experimental conditions for this study.

Table 1. Experimental conditions.

Experimental Conditions	Typical	Range
Flow rate, ml/min	500	200-700
Oxygen content,% (v/v)	3	3-10
H_2O content, % (v/v)	2	0-5
[SO_2], ppm[a]	400	200-700
[NO], ppm[a]	400	200-700
Capacitor-charging voltage, kV	50	20-50
Temperature (^{0}C)	100	100-250
GHSV[b], h^{-1}	30,000	20,000-30,000
Frequency, kHz	8.5	5-10

[a]ppm: per million, volumetric, [b]GHSV; gas hourly space velocity

The conversion efficiency of NO and SO_2 was calculated as follows;

$$\eta_{NO} = 100(c_{in,NO} - c_{out,NO})c_{in,NO}^{-1} \quad (1)$$

$$\eta_{SO_2} = 100(c_{in,SO_2} - c_{out,SO_2})c_{in,SO_2}^{-1} \quad (2)$$

Where $c_{in,NO}$ or c_{in,SO_2} are the pollutants initial concentration and $c_{out,NO}$ or c_{out,SO_2} are the pollutants concentration after treatment. The discharge power was calculated from the product of discharge voltage and the discharge current measured by voltage probe (Tektronix PPO201) and current probe (Tektronix PPO202) respectively, the specific energy density (SED) was determined as follows;

$$SED(JL^{-1}) = \frac{P(W)}{Q(L/min)} x60 \quad (3)$$

Where $P =$ discharge power and $Q =$gas flow rate

2.2. Catalyst preparation

The CeO_2/TiO_2 catalyst was prepared by impregnation method using an anatase type TiO_2 as catalyst support. The surface area of TiO_2 was 88.6 cm^2/g. Incipient wetness technique was used in

impregnation with an aqueous solution containing cerium nitrate, the solution was stirred electromagnetically for 30 minutes at room temperature, the sample was then kept in a water bath at 80^0C for 5hrs to raise its viscosity. Then dried in an oven at 100^0C for 12hrs, followed by calcination in air heating furnace at 500^0C for 7hrs.

2.3. Catalyst characterization

The N_2 adsorption-desorption experiment was performed using Micrometrics –ASAP 2020 HD88 instrument at -195.7^{0}C, to determine the surface area and adsorption pore size, the Brunauer-Emmett-Teller (BET) and Barrett-Joyner-Halenda (BJH) techniques were used respectively. In order to illustrate the X-ray diffraction (XRD) patterns, Rigaku D/max 2550PC system, X-ray diffractometer with CuKα radiation source in the 2θ range of 10^0 to 80^0 with a step length of 0.026^0 and a step time of 147s was used. Temperature programmed reduction with H_2 (H_2-TPR) was performed in a quartz micro reactor (PCA-1200), 100mg sample of the catalyst was used. First, the sample was pre-treated under an air flow at 500^0C for 1 hour, followed by purging with N_2 at 500^0C for 1 hour, then it was cooled down to room temperature for approximately 20mins, the flow of 6% H_2 in N_2 at a flow rate of 40ml/min was then switched into the system, then heated from room temperature at a rate of 10^0C/min to 820^0C. The amount of H_2 uptake during the reduction was measured by a thermal conductivity detector (TCD) which was calibrated by the quantitative reduction of CuO to the metallic copper.

The surface of CeO_2/TiO_2 physical chemical effects were characterized by scanning electron microscopy using Phenom pure desktop scanning microscope (model-PM 100 015) with an acceleration voltage 10kV.

3. Results and discussion.

3.1. N_2 adsorption-desorption analysis

The specific surface area was calculated by the BET method from the adsorption data obtained in a relative pressure (p/p_o) range of 0.011-0.140, the total pore volume was measured from the quantity of N_2 adsorbed at $p/p_o \approx 0.99$, the physico-chemical properties of CeO_2/TiO_2 are summarized in the Table 2. The CeO_2 loading was 20%.

Figure 2. Shows the N_2 adsorption-desorption isotherms, the N_2 adsorption/desorption profile of the CeO_2/TiO_2 catalyst can be assigned to type IV isotherm, it shows a hysteresis loop due to capillary condensation, which is a typical occurrence of a mesoporous material. The smaller the particle size results in increased surface area and change in its morphology hence providing a larger number of reactive edge sites.

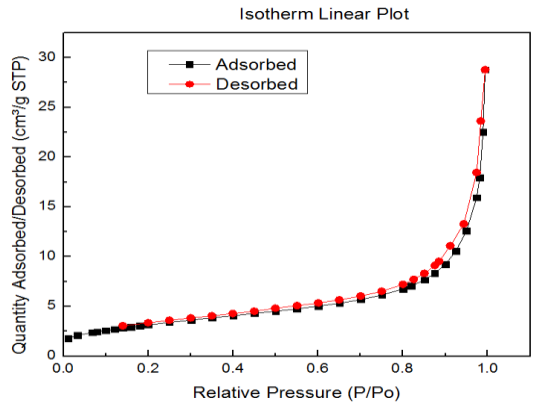

Figure 2. N_2 Adsorption/desorption isotherms.

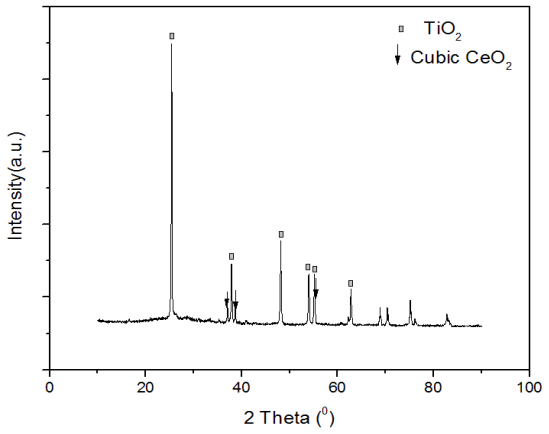

Figure 3. XRD pattern.

Table 2. Properties of CeO_2/TiO_2

Textual properties				
S_{BET}[a] (m^2/g)	S_{lang}[b] (m^2/g)	V_p[c] (cm3/g)	Pore size[d] (nm)	M_c[e] (nm)
72.12	18.6018	0.2464	11.9432	18.5736

[a] BET surface area is calculated over the pressure range 0.011-0.140 at $p/p_o \approx 0.99$
[b] Langmuir surface area
[c] Total pore volume
[d] pore size diameter
[e]Mean Crystallite size of TiO2

3.2. X-Ray diffraction (XRD)

X-ray powder diffraction (XRD) was carried out to show the catalyst structure. Figure 3 shows the XRD patterns of the CeO_2/TiO_2 catalysts prepared by impregnation technique, the crystalline phase of cubic CeO_2 was apparent, this suggests that more ceria crystallites were present, in addition, it can be seen in Figure 3 the diffraction peaks at $2\theta = 25.41^0$, 37.88^0, 48.12^0. 53.97^0, 55.15^0, 62.75^0 assigned to anatase TiO_2 (PDF-#21-1272), the sharpness and the relative density of main anatase TiO_2 peak (101) was relatively larger which means that the interaction between ceria and titania was weakest, this observation tally with the result achieved by X. Gao et al. [17]. Debye-scherrer equation was used to compute the mean crystallite size of anatase TiO_2 shown in Table 1 [18].

$$d = \frac{0.89\lambda}{\beta - \beta_0 \, Cos\, \theta} \quad (4)$$

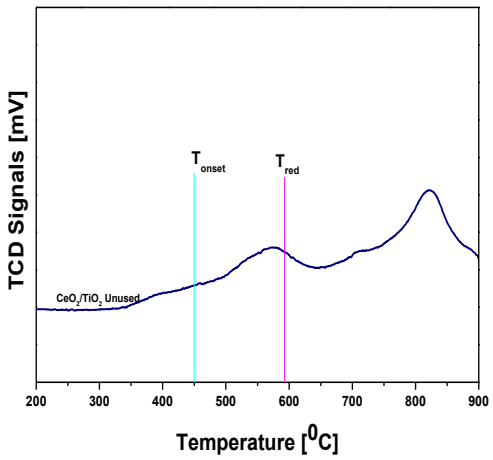

Figure 4. H_2-TPR profile of CeO_2/TiO_2 catalyst.

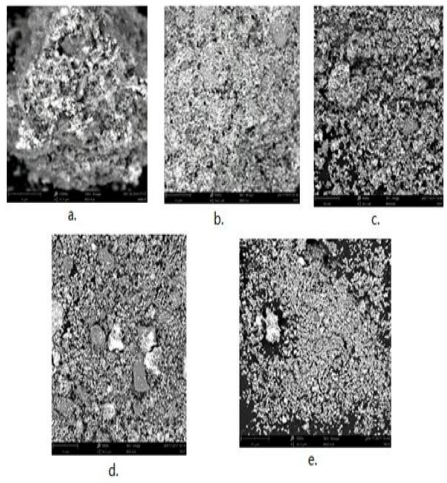

Figure 5. 200µm SEM images of CeO_2/TiO_2 surface before and after DBD reaction after 8hrs (5000x) a. Unused b. at 100^0C c. 150^0C, d. 200^0C e. 250^0C.

Where d- is the average volume diameter of crystallite, λ-wavelength of the incident X-ray, θ-incidence angle of X-rays with respect to the sample surface, β-the peak width at half peak height (radians) and β_0-the instrumental line broadening. The related diffractions patterns for TiO_2 anatase phase and cubic CeO_2 are as indicated in PDF-ICDD 21-1272) and PDF-ICDD 340394 respectively. Weak peak intensity suggests the lower crystallinity and smaller crystallite size due to metal oxide loading, which is helpful for the heterogeneous catalytic reactions. The characterization was performed before and after the NTP-CeO_2/TiO_2 tests and the same XRD results were obtained.

3.3. H_2-Temperaure Programmed Reduction (H_2-TPR)

The reducibility of metal supported catalyst is one of the most important factors affecting catalytic oxidation reaction. The TPR profile shown in Figure 4 indicates a reduction peak (T_{red}) at 591^0C, in this study, the T_{red} was taken as a measure of reducibility of CeO_2/TiO_2, the lower the T_{red} the stronger the redox ability of the catalyst. There was only one reduction peak, the onset temperature (T_{onset}) was about 450^0C, this is likely assigned to the reduction of non-stoichiometric ceria of type Ce^{3+}-O- Ce^{4+}, the reduction of bulk ceria did not take place in the temperature range 300^0C- 600^0C, since it occurs only above 750^0C. The results show that the reducibility of CeO_2/TiO_2 depends on the particle size and the dispersion of metal oxide on the surface of the catalyst [18].

3.4. Scanning Electronic Microscopy (SEM)

The SEM was carried out to compare the physical-chemical effects of plasma on CeO_2/TiO_2. It was observed that after plasma operation, the catalyst surface was affected as shown in Figure 5. As the temperature was varied from 100^0C-250^0C the catalyst surface changes, the same was observed by J.V Durme et al. [3] who attributed this change in catalytic structure to the following; NTP discharge increase dispersion of catalytic components, NTP demonstrated that the stability and CeO_2/TiO_2 catalyst activity are influenced during the plasma-catalytic process, as a result of plasma catalyst interactions, less parent Ti-O bonds are found on TiO_2 surfaces [3, 19], it can be deduced that CeO_2/TiO_2 catalyst exposure to plasma cause specific area enhancement and change of catalytic structure. It was realized that the granularity of the grain on the surface of CeO_2/TiO_2 catalyst reduces in size and the dispersion was more uniform after NTP discharge exposure, leading to ultrafine particles formation with higher surface area and less perfect crystal lattice having large number of vacancies, these physical changes detected induced a higher catalytic activity [20-21], surface area is known to be essential fundamental for thermal heterogeneous catalytic process for extensive reasons, high surface area in catalyst provides more active sites [22-28] justifying the synergetic effect of plasma-CeO_2/TiO_2 catalyst system. B.M Reddy at al. [29] shown that the catalytic properties of CeO_2/TiO_2 mainly depend on different factors such as; particle size, structural defects/distortion (lattice), chemical non-stoichiometry and phase modification.

4. NO conversion mechanism.

The high voltage used cause a shift in electron energy distribution in the non-thermal plasma to higher energies resulting to increased dissociation, excitation, and ionization rates, the association of ambient gas molecules produces free radicals plus other active species shown in the following reactions; [3,5,21,24]

$$e^*+O_2 \rightarrow e+2O \quad (R1)$$
$$e^*+N_2 \rightarrow e+2N \quad (R2)$$
$$O+O_2+M \rightarrow O_3+M \quad (R3)$$
$$O+NO+M \rightarrow NO_2+M \quad (R4)$$
$$O_3+NO \rightarrow NO_2+O_2 \quad (R5)$$
$$N+NO \rightarrow N_2+O_2 \quad (R6)$$
$$N+O \rightarrow NO \quad (R7)$$

The active species such as N, O atoms and O_3 molecules are produced through electron impact dissociation of N_2 and O_2 in the plasma reactor, these atoms plays a key role in the oxidation or reduction reaction with NO to produce N_2 or NO_2 as follows [8,19-21]

Increasing SED leads to increase reactive species that in turn leads to the conversion of more NO molecules from the gas stream, explaining the observation that NO conversion rate increases with increase in specific energy density as illustrated in Figure 7. Some of the chemically active species reacts with each other;

$$O+O_3 \rightarrow 2O_2 \quad (R8)$$
$$O+O \rightarrow O_2 \quad (R9)$$
$$N+N \rightarrow N_2 \quad (R10)$$
$$N+O \rightarrow NO \quad (R11)$$
$$N^*+O_2 \rightarrow NO+O \quad (R12)$$
$$O+NO_2 \rightarrow NO+O_2 \quad (R13)$$
$$N+OH \rightarrow NO+H \quad (R14)$$
$$NO+OH \rightarrow HNO_2 \quad (R15)$$
$$HNO_2+OH \rightarrow NO_2+H_20 \quad (R16)$$
$$NO+HO_2 \rightarrow NO_2+OH \quad (R17)$$
$$NO_2+OH \rightarrow HNO_3 \quad (R18)$$

Metastable excited state nitrogen atoms (N*) leads to undesirable reaction with oxygen resulting to formation of NO [8, 19, 21]

The conversion of NO by ground state atomic nitrogen as shown in reaction R6 is mainly encountered by NO formation as indicated in reaction R14, atomic oxygen is also involved in undesired reaction with NO_2, leading to the formation on NO [21].

It should be noted that only selected chemical reactions are listed in this study, these are the main reactions which are helpful in explaining the main observations, a comprehensive list of chemical reactions plus their rate constants are provided in various literature [21,23, 24, 27], NO conversion is usually explained on the foundation of free radical reactions, however, there is a possibility of NO conversion through ionic reactions especially those that may be initiated by the oxidation of NO to NO^+ cannot be ruled out. The other chemical reactions for conversion of NO in the presence of water vapor can be expressed as;

4.1. Effect of temperature on NO conversion

To compare the conversion of NO, catalyst, NTP and a combination of both catalyst and NTP were investigated, simulated gas was heated to 100^0C, 150^0C, 200^0C and 250^0C respectively, the inlet gas stream contains 400ppm NO,50ppm NO_2 and 3% oxygen content with Argon as the carrier gas, the results was as shown in Figure 6. When the catalyst alone was used in the reactor, as temperature increases from 100^0C to 250^oC the oxidation efficiency of NO increases gradually from 5% with the maximum efficiency of 6% achieved at 250^oC. When NTP was used without the catalyst the highest conversion efficiency attained was 71% at 250^0C with the lowest NO Conversion efficiency of 62% recorded at 100^0C when the specific energy density was 91J/L. Temperature variation can affect NO conversion by dielectric barrier discharge with regards to the following aspects; gas reaction time, reaction rate coefficients and E/N [23]. E/N, which is used to determine the electron energy, depends on the electric field strength divided by gas density and affects gas discharge in terms of occurrence frequency and the intensity. To evaluate E/N, the electric field strength (E) is proportional to the applied voltage given that the plasma reactor parameters remain constant. Moreover, the gas density (N) given by Equation 5.

$$\mathrm{N} = P'/RT \tag{5}$$

Where P'-the gas pressure, R-gas constant, T-temperature.

Consequently, an increase in temperature will result to a decrease in gas density(N), for that reason, an increase in E/N under the test conditions. An increase in E/N leads to more energy being transferred to particles generated by the discharge, which improves radical formation reactions R1-R4 involving electrons and molecules. Increasing temperature from 100^0C-250^0C much more atoms and radicals are produced from dissociation of N_2, O_2 and NO, thereby promoting the reactions for NO conversion. Temperature is a crucial factor affecting the reaction rate constant, which dominates the chemical kinetics in gas- phase reactions [23, 24, 26, 27].

A remarkable conversion was realized when catalyst and NTP was used, the highest conversion was 75% at 100^0C but increase in temperature the conversion reduces, hence preliminary conclusion was that NTP affects the catalyst performance, and further investigation of the effect of NTP in terms of SED was carried out in subsequent sections.

4.2. Plasma assisted catalytic oxidation of NO using CeO_2/TiO_2

Figure 7a Shows the effect of SED on the performance of the plasma-catalytic process in terms of NO concentration, clearly NO concentration decreases from 177ppm to 51ppm with SED increasing when NTP was used together with the catalyst, while NO concentration decreased from 184ppm to 108 ppm with the increase in SED, similar to results reported by Y.S. Mok et al. [5]. Increasing the specific energy density intensify the electric field of the discharge and increases the generation of highly energetic electrons and chemically active species which can initiate a variety of different reactions, therefore, resulting to increase in the NO conversion [26, 27].

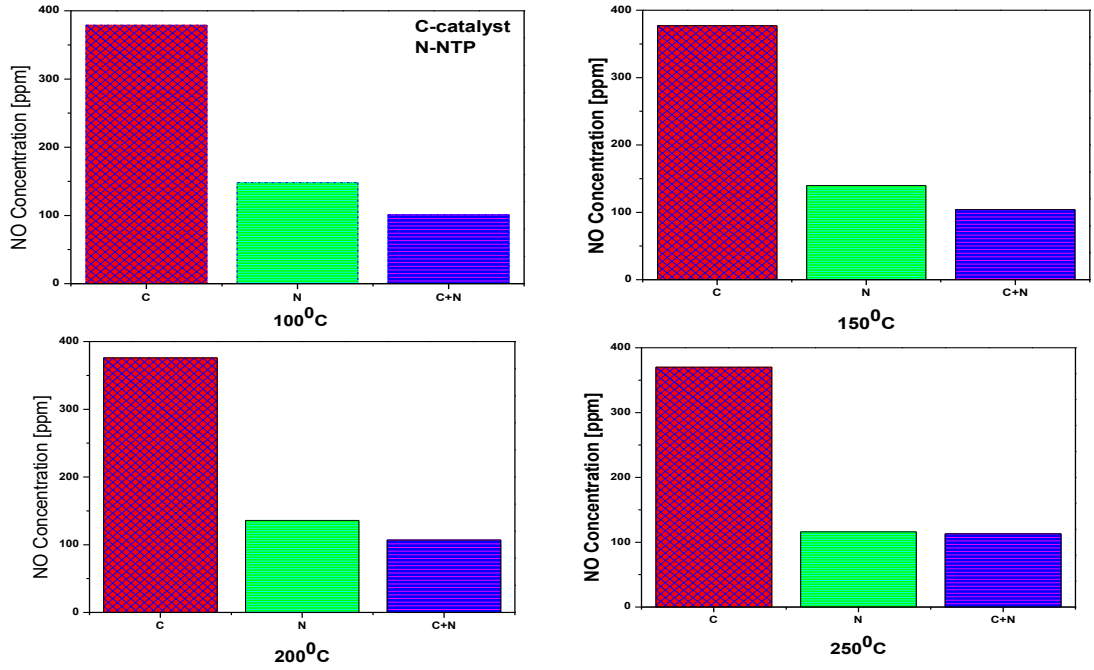

Figure 6. Effect of temperature on the concentration of NO at the reactor outlet (Inlet NO-400ppm, inlet NO_2-50ppm, GHSV=30,000h^{-1}, Oxygen 3%, balance gas -Ar).

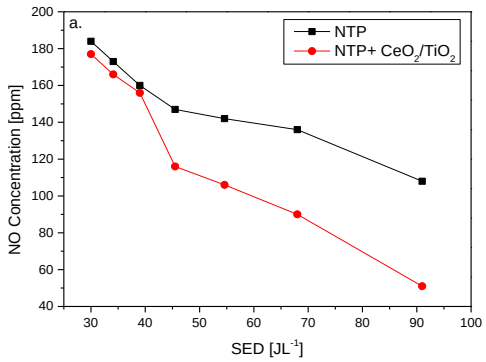

Figure 7a. Effect of specific energy density on the concentration of NO at the reactor outlet (Inlet NO-400ppm, inlet NO_2-50ppm, T=100^{0}C, 3% Oxygen, balance gas Ar).

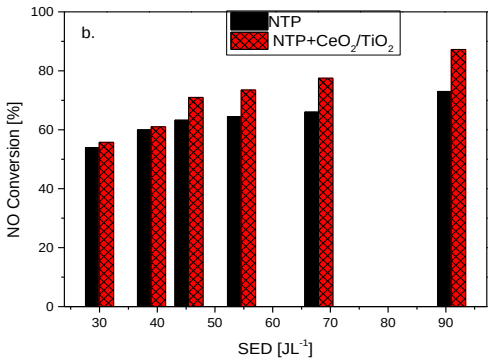

Figure 7b. Effect of specific energy density on the concentration of NO at the reactor outlet (Inlet NO-400ppm, inlet NO_2-50ppm, T=100^{0}C, 3% Oxygen, balance gas Ar).

Figure 7a can be redrawn for plasma catalytic process in terms of specific energy density (SED) which is the ratio of power delivered to total flow rate. Converting y-axis to conversion efficiency as shown in Figure 7b. The maximum NO oxidation efficiency of 87% was achieved within the tested SED range when Catalyst was used with NTP. The increase in NO oxidation with SED can also be explained in terms of the flow rate, since flow rate is inversely proportional to SED, decreasing the flow rate from 900ml/min to 300ml/min increases SED hence increasing oxidation efficiency from 56% to 87% because the exposure of gas to the discharge area with electric field decreases [9].

4.3. Effect of SO_2 on NO conversion over CeO_2/TiO_2

The effect of SO_2 on NO conversion was investigated, the experimental feed gas composed of NO (400ppm), 3% oxygen, Argon as a balanced gas and SO_2 concentration varied. The results of 10 hours' test performed at 100^0C is shown in Figure 8.

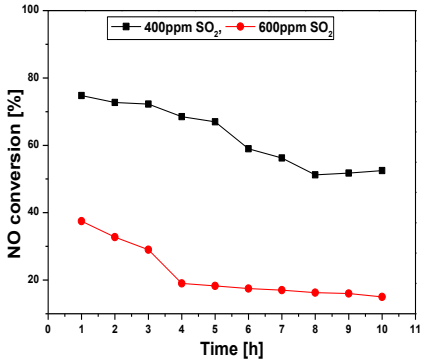

Figure 8. Effect of SO_2 on NO conversion over CeO_2/TiO_2, Reaction condition: (inlet NO=400ppm, O_2=3%, Q=500ml/min, T=100^0C, GHSV=30,000h^{-1}, balance gas-Ar).

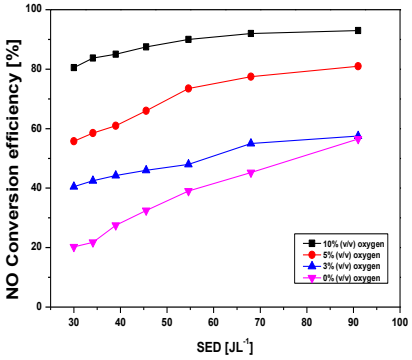

Figure 9. Effect of oxygen content on NO conversion over CeO_2/TiO_2, reaction condition: inlet NO=400ppm, inlet NO_2=50ppm, T=100^0C, balance gas –Ar.

The variation of NO conversion over the catalyst under different SO_2 concentration was investigated and illustrated in Figure 8. When 400ppm of SO_2 was added to the gas feed stream, the NO conversion decreased from 74% to 55%, for the first 3 hours NO conversion had negligible change, but subsequently decreasing more rapidly from 72% to 52% in 7hours. When 600ppm of SO_2 was used the NO conversion decreased more rapidly 38% to 14%, this may be attributed to XRD results obtained, the adsorption of SO_2 on the CeO_2/TiO_2 was less suppressed due to weak interaction between ceria and titania and also different Ce species on catalyst surface [30] as earlier shown by the XRD results, the sharp peak and the relative density of the main anatase TiO_2 peak (101) was relatively larger which means that the interaction between ceria and Titania was weakest.

4.4. Effects of oxygen content on NO conversion

NO conversion under different oxygen content was investigated with other variables kept constant, Figure 9 shows the effect of oxygen content on NO conversion, the NO conversion can be elucidated as a competition between oxidation and reduction [5] increasing the oxygen content from 0% to 10% increases the NO conversion efficiency due to increase in production of oxidation radicals.

The NO conversion rate increases with the increase in oxygen content, as a result of large amount of activated oxygen to oxidize NO to NO_2, the highest conversion efficiency of 93% was attained at 91J/L when oxygen content was 10 % as shown in Figure 9, The NO conversion by O_2 based active species reactions R4 and R5 is partially encountered by NO formation reaction R12 and the reverse reaction R13, therefore, in the absence of oxygen content the NO removed as shown in reaction R6 and NO formation does not take place reactions R11 and R13, this explains why the conversion of NO increases as oxygen content increases from 0% to 10% [21, 22]. In the presence of oxygen, the nitrogen active species in NO conversion as reaction R6, N is mostly encountered by the effect of N* in reaction R12. The removal of NO by oxygen based active species illustrated in reaction R4 is partially encountered by the reverse reaction R13 or formation of NO, hence oxygen based active species are the major contributors to NO conversion when oxygen is present. The oxidation of NO to NO_2 in the plasma reactor improves the catalyst performance, since NO_2 conversion is better than NO conversion near the catalyst [9]. It can be concluded that the main reactions for the conversion of NO are the oxidation at oxygen rich conditions while reduction dominates in the opposite condition [5].

4.5. Effect of water vapour content on NO Conversion

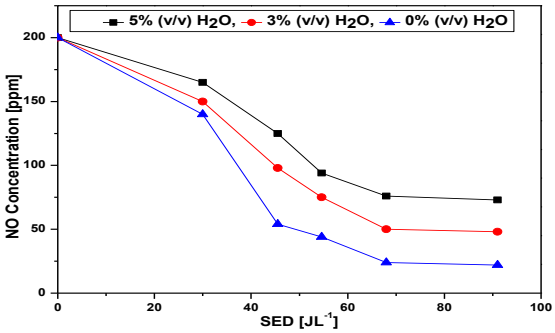

Figure 10. Effect of water vapor content on NO conversion, reaction condition: Inlet NO=200ppm, inlet NO_2=50ppm, T=100^{0}C, balance gas- Ar.

The variation of NO concentration with water vapor content is illustrated in Figure 10. It was expected that increasing water vapor content would result to increase in NO conversion unless other conditions were changed, since water vapor provides OH and HO_2 radicals capable of oxidizing NO to NO_2, however, the results obtained were contrary to the expectation. The results obtained can be explained from the following aspect. OH radicals produced from H_2O can deplete ozone as follows [5, 31];

$OH+O_3 \rightarrow HO_2+O_2$ (R19)

Ozone produced during dielectric barrier discharge process is the most important species for the oxidation of NO [23, 24].

4.6. Effect of flow rate on NO conversion in the plasma/CeO_2/TiO_2

The effect of flow rate on NO conversion is shown in the Figure 11, the flow rate was varied from 400ml/min to 700ml/min at constant applied voltage and the experiment carried out at different oxygen contents. The inlet concentration of NO and SO_2 was kept at 400ppm

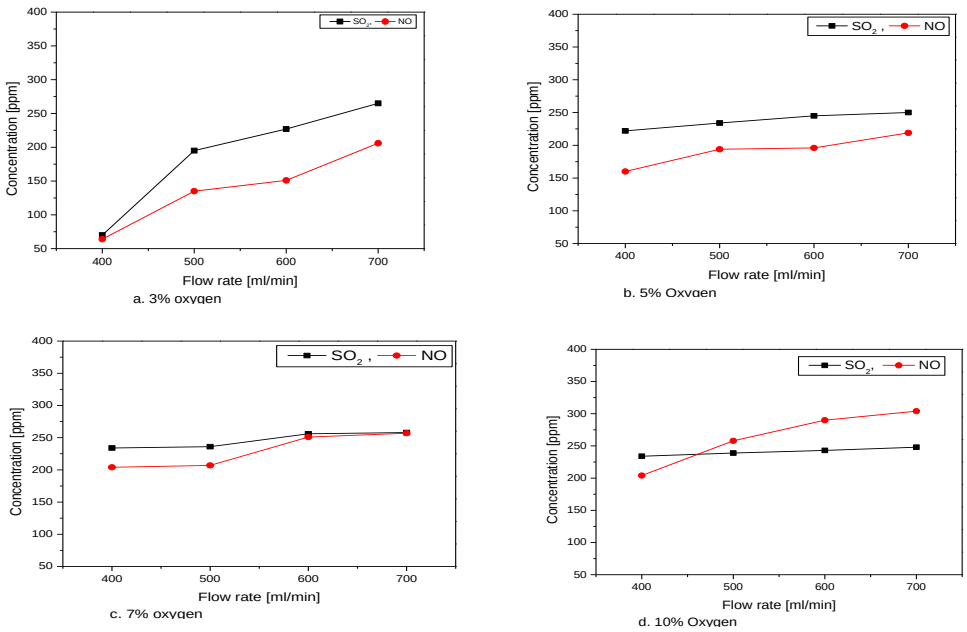

Figure 11. Effect of flow rate on NO conversion, reaction condition: (inlet NO=400ppm, SO_2=400ppm, inlet NO_2=50ppm, T=100^{0}C, 3% H_2O, balance gas –Ar).

It was observed that outlet NO concentration increased with increasing flow rate, the NO conversion efficiency decreased from 84% at a flow rate of 400ml/min to 48.5% efficiency at 700ml/min, at the 3% oxygen while the conversion efficiency of SO_2 attained at a flow rate of 400ml/min and 700ml/min was 83% and 33.75% respectively. The conversion efficiency of NO was greater than SO_2 conversion efficiency when the oxygen content was 3%, 5% and 7% but when 10% water content was used the SO_2 conversion efficiency was higher than that of NO conversion efficiency from 500ml/min to 700ml/min flow rate. The SO_2 conversion efficiency achieved was 83%. Generally, the conversion efficiency decreases with the flow rate. The OH radicals performs a leading role in converting SO_2 and NO to their respective acids, the OH radicals are produced from the reaction of water molecule with metastable O atom. The presence of SO_2 serves to lower the energy necessary for oxidation of NO by converting OH to HO_2, when NO is oxidized by HO_2, the OH radicals is regenerated as illustrated in the reactions R20-R27.

$$OH+SO_2 \rightarrow HSO_3 \quad (R20)$$
$$HSO_3+O_2 \rightarrow HO_2+SO_3 \quad (R21)$$
$$SO_2+HO_2 \rightarrow HO+SO_3 \quad (R22)$$
$$HSO_3+OH \rightarrow HSO_4 \quad (R23)$$
$$HO_2+NO \rightarrow NO_2+OH \quad (R24)$$
$$NO+OH \rightarrow HNO_2 \quad (R25)$$
$$HNO_2+OH \rightarrow NO_2+H_2O \quad (R26)$$
$$NO_2+OH \rightarrow HNO_3 \quad (R27)$$

The main reaction for NO conversion is oxidation of NO to NO_2 and HNO_2, finally, in the presence of water, NO and NO_2 can be converted to acidic products by reactions R25 and R27 while the major reactions for SO_2 conversion are reactions R20-R23.

5. Conclusions

In this work CeO_2/TiO_2 catalyst characterization has been investigated for the conversion of NO, the combination of NTP with CeO_2/TiO_2 catalyst significantly enhances the oxidation of NO. The maximum NO conversion efficiency of 93% was achieved when CeO_2/TiO_2 was directly packed into the DBD reactor at SED 91 J/L with oxygen content 10%. Using CeO_2/TiO_2 alone in the reactor shows the lowest oxidation efficiency, this can be attributed to the weak surface oxygen activity on the surface of CeO_2/TiO_2 as illustrated by the high reduction temperature (above 750^0C). It was realized that the reducibility, surface area and pore properties of the catalyst plays a dominant role in plasma catalytic conversion of NO. Moreover, the effect of oxygen content has been conducted to show that plasma catalytic conversion efficiency of NO increases with increasing oxygen content for the range 0% -10% oxygen content. SO_2 has a great influence on the CeO_2/TiO_2 catalytic process under the test conditions since it affects CeO_2/TiO_2 performance. Lastly, increasing water vapor content decreases NO conversion rate which serves as the evidence that ozone plays a crucial role in DBD oxidation chemistry.

Acknowledgement

The authors are grateful for the financial support of Key Project National Science Foundation of Tianjin (18JCZDJC39800), The project science and technology of Tianjin (18ZXSZSF00040) and the project of science and technology of Tangshan (18130211A).

References

[1] Matsumoto T,Wang D,Namihira T,Akiyama H Non-thermal plasma technic for air pollution control, Air Pollution"-A comprehensive perspective **3** 215-234
[2] Ighigeanu D,Martin D, Calinescu I,Zissulescu E, Oproiu C, Manaila E, Cracium G 2006 VOC removal by microwave electron beam and catalyst technique" *Environmental physics conference* **2** 101-112
[3] Durme J V,Dewulf J,Leys C, Langenhove H V 2008 Combining non-thermal plasma with heterogeneous catalysis in waste gas treatment" *Applied Catalysis B: Environmental* **78** 324-333

[4] Srinivasan A D, Rajanikanth B S, Mahapatro S 2009 Corona treatment for NOx reduction from stationary diesel engine exhaust impact of nature of energization and exhaust composition" Electrostatics Joint Conference, Boston University,June 16-18 **1** 26
[5] Mok YS., Lee H W, Hyun Y J, Ham S W, Kim J H, Nam I S 2001 *Korean J. Chem Eng* **18(3)** 308-316
[6] Dors M, Mizeraczyk J 2004 *J. of Catalysis Today* **89** 127-133
[7] Huu T P, Gil S, Costa P D, Giroir-Fendler A, Khacef A 2015 Catalysis Today **257** 86-92
[8] Park S Y,Deshwal B R, Moon S H 2008 *J. of Fuel proc Technology* **89** 540-548
[9] Talebizadeh P, Babaie M, Brown R, Rahimsadeh H, Ristovski Z, Arai M 2008 *J. of Renewable and Sustainable energy* . Rev 40
[10] Frank N R 1995 J. of Radiation Physics and Chemistry **45** 989-1002
[11] Nakagawa Y, Kawauchi H 1998 *Jpn. J. Appl. Phys* **37** L91-L93
[12] Talebizadeh P, Babaie M, Brown R, Rahimzadeh H, Ristovski Z, Arai M *2014 J. of Renewable and Sustainable energy reviews* Dec. 2014.
[13] Fridman A, Chirokov A, Gutsol A 2005 *J. of Physics D: Applied Physics* **38** R1
[14] Whealton J H, Hansen G R,Storey J M, Raridon R J,Armfield J S, Bigelow T S 1997 Non-thermal plasma exhaust aftertreatment" a fast rise-time concept SAE
[15] Penetrante B M Application of pulsed power and power modulation to the non- thermal plasma treatment of hazardous Gaseous wastes, UCRL-JC-112501
[16] Orlandini I, Riedel U 2000 *J. Phys. D: Appl. Phys.* **33** 2467-2474
[17] Gao X, Jiang Y, Fu Y, Zhong Y, Luo Z, Cen K 2010 *J. of catalysis communications* **11** 465-469
[18] Zhu X, Gao X, Yu X, Zheng C, Tu X 2015 *J. of catalysis today* **256** 108-114
[19] Y.S. Mok, S.W Ham 1998 Conversion of NO to NO_2 in air by a pulsed corona discharge process, Chem. Eng. Sci **53-9** 1667-1678
[20] Mizuno A, Clements J S, Davies R H 1986 *IEEE Trans. Ind. Appl* **516**
[21] Malik M A, Kolb J F, Sun Y, Schoenbach K H 2011 *J. of Hazardous material* **197** 220-228
[22] Jiang N, Shang K F, Lu N, Li H, Li J, Wu Y 2016"High Efficiency Removal of NOx from flue gas by multitooth wheel cylinder corona discharge plasma facilitated selective catalytic reduction processes. *IEEE Transactions on plasma science* 44-11.
[23] Wang T, Sun B 2016 *J. of Fuel Processing Technology* **144** 109-114
[24] Dong L M, Lan S, Yang J X, Chi X C 2003 Plasma chemical reaction for nitric oxide and sulfur dioxide in corona discharge reactor, annual report conference on electrical insulation and dielectric phenomenon.
[25] Xu W, Yu Y, Zhang C,He H 2008 *J. of catalysis communication* **9** 1453-1457
[26] Patil B S, Cherkasov N, Lang J, Ibhadon A O, Heseel V, Wang Q 2016 *J. of applied catalysis B; Environmental* **194** 123-133
[27] Zhang X, Lee B J, Im H G, Cha M S 2016 Ozone production with dielectric barrier discharge; effects of power source and humidity, *IEEE transactions on plasma science* **44**.
[28] Marrotta E, Paradisi C 2009 *J. Am. Soc. Mass spectron* **20** 697-707
[29] Reddy B M, Khan A 2005 J. of Catalysis surveys from Asia **9**
[30] Tian J, Sang Y, Zhao Z, Zhou W, Wang D, Kang X, Liu H, Wang J, Chen S, Cai H, Huang H 2013 *J. of photo catalysis* **22** 3864-3872
[31] Atkinson R, Baulch D L, Cox R A, Hampson R F, Kerr J A, Troe J 1992 "Evaluated Kinetic and Photochemical Data for Atmospheric Chemistry: Supplement IV", *J. Phys. Chem*. Ref. Data **21** 1125